MAGNETOHYDRODYNAMICS Vol. 40 (2004), No. 2, pp. 203–212

STABILITY OF ALUMINUM REDUCTION CELLS WITH MEAN FLOW

A. Kurenkov[1], *A. Thess*[2], *O. Zikanov*[3],
M. Segatz[4], *Ch. Droste*[4], *D. Vogelsang*[4]

[1] *Department of Hydromechanics and Hydraulics, Technical University of Darmstadt, 64287 Darmstadt, Petersenstrasse 13, Germany*
[2] *Department of Mechanical Engineering, Ilmenau University of Technology, P.O.Box 100565, 98684 Ilmenau, Germany*
[3] *University of Michigan - Dearborn, Department of Mechanical Engineering, Dearborn, MI, 48128-1491, USA*
[4] *Hydro Aluminium-Technologie GmbH, 53117 Bonn, Germany*

We report results of the linear stability analysis undertaken to investigate the effect of the mean flow of liquid metal on the stability of aluminum reduction cells. A simplified model of the cell is considered that consists of thin layers of aluminum and cryolite superimposed in an infinite horizontal channel with electrically non-conducting walls. A vertical uniform magnetic field and an electric current are applied in the opposite directions. In the basic steady state, a uniform flow of aluminum is assumed, while cryolite is at rest. The onset of the instability is caused by the action of two different mechanisms. The first is the Kelvin–Helmholtz instability of the mean flow. The second, essentially the MHD mechanism, is a consequence of destabilizing electromagnetic (Lorentz) forces produced by nonuniformities of the electric current due to interface deflections. We use the shallow water approximation and solve the problem for the cases of pure Kelvin–Helmholtz (zero magnetic field) and pure MHD (zero mean flow) instabilities and for the general case. We compute the stability chart and derive the parameters that determine the stability threshold. It is found that, while both playing a destabilizing role, the instability mechanisms do not affect each other. In particular, a uniform mean flow changes the direction of propagation of interfacial waves but leaves the MHD stability threshold unaltered.

Introduction. Although the mechanism of MHD instabilities in aluminum reduction cells has being investigated for more than 30 years, the complexity of the problem is still challenging. Design and operation of cells with higher amperage and continued demand for lower energy consumption requires both a detailed theoretical understanding of the underlying physical principles and accurate numerical models. The development in this direction went a long way from a basic criterion for the magnetic field [1], over MHD stability analysis [2] and shallow water approximations [3], [4], to detailed models [5] of instabilities, including the physical effects of the oscillating magnetic field and cavity size, and many geometric details such as anode channels and ledge profile. The interaction between the horizontal perturbations of electric currents and the vertical component of unperturbed magnetic field has been identified as the most significant mechanisms of the MHD stability.

Based on this mechanism, the linear stability analysis [6], [7] leads to a wave equation for the interface deviation

$$\frac{\partial^2 \boldsymbol{\eta}}{\partial t^2} + \Omega^2 \boldsymbol{\eta} = \epsilon K \boldsymbol{\eta} \tag{1}$$

Here $\boldsymbol{\eta}$ is the vector of amplitudes of Fourier interface modes, the diagonal matrix Ω contains gravitational frequencies of interface oscillations, K is the matrix with the

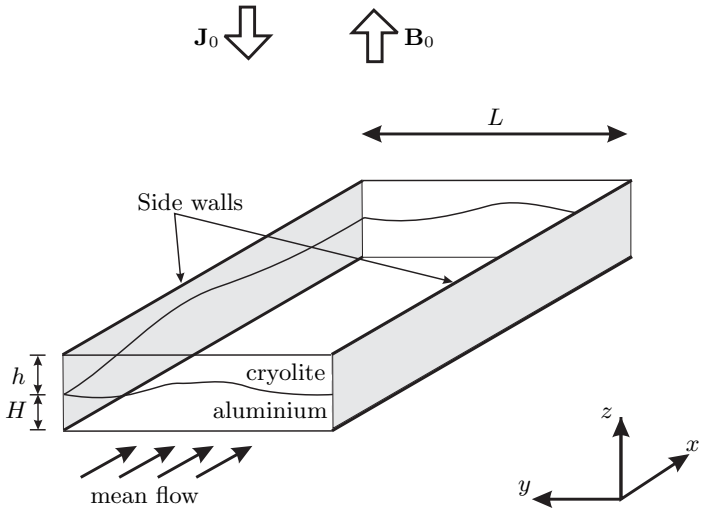

Fig. 1. Schematic presentation of the model. In the basic steady state, a uniform flow (mean flow) in aluminum is assumed, while cryolite is supposed to be at rest.

magnetic interaction coefficients, and the parameter ϵ is a dimensionless measure of the relative magnitude of gravitational and magnetic forces. At vanishing electric current or magnetic field ($\epsilon = 0$), the solution of the eigenvalue problem (1) reduces to the standard gravitational wave spectra with all real eigenvalues. At increasing current density and magnetic field or decreasing anode-cathode distance (ACD) or density difference, the solution is modified so that pairs of eigenvalues degenerate to form complex-valued eigenmodes, indicating the onset of the MHD instability. The shape of the unstable interface modes is always that of propagating waves, while the real eigenmodes are just deformed gravitational standing waves.

In the aluminum cells, the most dangerous instability mode is, therefore, a rotating single-crest wave. It must be stressed, however, that this model of instability does not take into account the significant mean flow in both layers produced by the Lorentz force. This issue is addressed in the present paper. In particular, we investigate the mutual influence of two types of instability, one originating from horizontal electric currents in aluminum (MHD-instability), and the other caused by the mean flow (Kelvin–Helmholtz instability [8], [9]).

We consider the simplified model of an aluminum reduction cell sketched in Fig. 1. The cryolite layer is superposed over the aluminum one in an infinite horizontal channel of width L. We assume that both fluids are inviscid. The flow in the aluminum is supposed to be uniform $\mathbf{U}_\mathrm{a} = U_0\mathbf{e}_x$. The cryolite is initially at rest. A vertical uniform magnetic field $\mathbf{B}_0 = B_0\mathbf{e}_z$ and a uniform electric current $\mathbf{J}_0 = -J_0\mathbf{e}_z$ are applied.

1. Basic equations.

1.1. Governing equations and basic flow. Our model is based on the shallow water approximation [10]. The approximation rests on the assumption that the layer thicknesses are small, i.e.,

$$h, H \ll L, \lambda, \tag{2}$$

where λ is the typical length scale of interfacial perturbations, and h and H are the thicknesses of cryolite and aluminum layers, respectively.

Taking into account the Lorentz force in the aluminum $\mathbf{F}_\mathrm{a} = -\sigma_\mathrm{a} B_0 \nabla_\perp \phi$ due to the interaction of the electric current perturbation $\mathbf{j}_\mathrm{a} = -\sigma_\mathrm{a} \nabla\phi$ with the magnetic field $B_0 \mathbf{e}_z$, the nonlinear shallow water equations, governing the fluid motions, can be written as [11]

$$\frac{\partial \mathbf{u}_\mathrm{a}}{\partial t} + (\mathbf{u}_\mathrm{a} \cdot \nabla)\mathbf{u}_\mathrm{a} = -\frac{\nabla p}{\rho_\mathrm{a}} - g\nabla\eta - \sigma_\mathrm{a}\frac{B_0}{\rho_\mathrm{a}}\nabla_\perp\phi \tag{3}$$

$$\frac{\partial \mathbf{u}_\mathrm{c}}{\partial t} + (\mathbf{u}_\mathrm{c} \cdot \nabla)\mathbf{u}_\mathrm{c} = -\frac{\nabla p}{\rho_\mathrm{c}} - g\nabla\eta \tag{4}$$

$$\frac{\partial \eta}{\partial t} + \nabla \cdot [(H+\eta)\mathbf{u}_\mathrm{a}] = 0 \tag{5}$$

$$\nabla \cdot [(H+\eta)\mathbf{u}_\mathrm{a} + (h-\eta)\mathbf{u}_\mathrm{c}] = 0 \tag{6}$$

$$\nabla^2\phi = -\frac{J_0\eta}{\sigma_\mathrm{a} H h} \tag{7}$$

where $\nabla_\perp = \mathbf{e}_x\partial/\partial y - \mathbf{e}_y\partial/\partial x$. The shallow-water approximation eliminates the z-dependence, so all equations are two-dimensional. Indices "a" and "c" refer to aluminum and cryolite respectively, $\mathbf{u}_\mathrm{a}(x,y,t)$ and $\mathbf{u}_\mathrm{c}(x,y,t)$ are the vertically averaged horizontal velocities in corresponding layers, $p(x,y,t)$ is the pressure at the interface $z = \eta(x,y,t)$, and $\phi(x,y,t)$ is the perturbation of the electrical potential. In the system (3)–(7), equations (3) and (4) are the momentum equations, (5) describes evolution of the interface, (6) imposes the mass conservation condition, and (7) provides the link between the deflection of the interface and perturbations of the electrical current.

The boundary conditions are

$$u_{ay} = u_{cy} = \frac{\partial\phi}{\partial y} = 0 \qquad \text{at } y = 0 \text{ and } y = L \tag{8}$$

The first two conditions are the conventional free slip conditions at the channel walls, while the last condition describes electrically non-conducting channel walls. Equations (3)–(7) admit an exact stationary solution

$$\mathbf{u}_\mathrm{a} = U_0\mathbf{e}_x, \quad \mathbf{u}_\mathrm{c} = 0, \quad p = \eta = \phi = 0, \tag{9}$$

whose stability with respect to infinitesimal perturbations we wish to investigate.

1.2. Evolution of small perturbations. We consider small perturbations $\mathbf{v}_\mathrm{a}$, $\mathbf{v}_\mathrm{c}$, p, η, ϕ superimposed upon the basic state (9). The linearized equations for the evolution of these perturbations are readily obtained from (3)–(7) as

$$\frac{\partial \mathbf{v}_\mathrm{a}}{\partial t} + U_0\frac{\partial \mathbf{v}_\mathrm{a}}{\partial x} = -\frac{\nabla p}{\rho_\mathrm{a}} - g\nabla\eta - \frac{\sigma_\mathrm{a} B_0}{\rho_\mathrm{a}}\nabla_\perp\phi \tag{10}$$

$$\frac{\partial \mathbf{v}_\mathrm{c}}{\partial t} = -\frac{\nabla p}{\rho_\mathrm{c}} - g\nabla\eta \tag{11}$$

$$\frac{\partial \eta}{\partial t} + U_0\frac{\partial \eta}{\partial x} + H\nabla \cdot \mathbf{v}_\mathrm{a} = 0 \tag{12}$$

$$U_0\frac{\partial \eta}{\partial x} + H\nabla \cdot \mathbf{v}_\mathrm{a} + h\nabla \cdot \mathbf{v}_\mathrm{c} = 0 \tag{13}$$

$$\nabla^2\phi = -\frac{J_0\eta}{\sigma_\mathrm{a} H h} \tag{14}$$

Defining $\chi = \nabla \cdot \mathbf{v}$ and $\omega = -\nabla_\perp \cdot \mathbf{v}$, and applying the operators $\nabla\cdot$ and $-\nabla_\perp\cdot$ to (10) and (11), we transform the first four equations into

$$\frac{\partial \chi_\mathrm{a}}{\partial t} + U_0\frac{\partial \chi_\mathrm{a}}{\partial x} = -\frac{\nabla^2 p}{\rho_\mathrm{a}} - g\nabla^2\eta \tag{15}$$

$$\frac{\partial \chi_c}{\partial t} = -\frac{\nabla^2 p}{\rho_c} - g\nabla^2 \eta \tag{16}$$

$$\frac{\partial \omega_a}{\partial t} + U_0 \frac{\partial \omega_a}{\partial x} = \frac{\sigma_a B_0}{\rho_a} \nabla^2 \phi \tag{17}$$

$$\frac{\partial \omega_c}{\partial t} = 0 \tag{18}$$

$$\frac{\partial \eta}{\partial t} + U_0 \frac{\partial \eta}{\partial x} + H\chi_a = 0 \tag{19}$$

$$U_0 \frac{\partial \eta}{\partial x} + H\chi_a + h\chi_c = 0 \tag{20}$$

The system can be further simplified by eliminating the pressure in (15) using (16), by eliminating χ_c using (20), and by noting that $\omega_c = 0$, if the vorticity of the cryolite is zero under the initial condition. Furthermore, equation (17) is not necessary to determine the stability threshold since ω_a is decoupled from the rest of the system. Finally, we obtain three equations

$$H\bar{\rho}\frac{\partial \chi_a}{\partial t} + \rho_a U_0 \frac{\partial \chi_a}{\partial x} = -g\triangle\rho\nabla^2\eta - \frac{\rho_c U_0}{h}\frac{\partial^2 \eta}{\partial x \partial t} \tag{21}$$

$$\frac{\partial \eta}{\partial t} + U_0 \frac{\partial \eta}{\partial x} + H\chi_a = 0 \tag{22}$$

$$\nabla^2 \phi = -\frac{J_0 \eta}{\sigma_a H h} \tag{23}$$

for the divergence of the aluminum flow χ_a, the interface deflection η and the electric potential ϕ. Here we denote $\bar{\rho} = (\rho_a/H) + (\rho_c/h)$ and $\triangle\rho = \rho_a - \rho_c$. To derive a boundary condition for η, we take the y-components of (10) and (11), use the first two conditions of (8) and eliminate the pressure obtaining

$$g\triangle\rho\frac{\partial \eta}{\partial y} = \sigma_a B_0 \frac{\partial \phi}{\partial x} \qquad \text{at } y = 0 \text{ and } y = L \tag{24}$$

This condition together with boundary condition (8) for the electric potential and stability equations (21)–(23) completes the formulation of the linear stability problem. It will be seen later that no boundary condition for χ_a is necessary.

1.3. Normal mode analysis and stability equations. We decompose the perturbation into normal modes according to

$$\begin{aligned} \chi_a &= \hat{\chi}_a(y) exp[ik(x - ct)] \\ \phi &= \hat{\phi}(y) exp[ik(x - ct)] \\ \eta &= \hat{\eta}(y) exp[ik(x - ct)] \end{aligned} \tag{25}$$

Substitution into (21)–(23) gives

$$ik(-\bar{\rho}Hc + \rho_a U_0)\hat{\chi}_a = -g\triangle\rho(D^2 - k^2)\hat{\eta} - ck^2 U_0 \frac{\rho_c}{h}\hat{\eta} \tag{26}$$

$$ik(-c + U_0)\hat{\eta} = -H\hat{\chi}_a \tag{27}$$

$$(D^2 - k^2)\hat{\phi} = -\frac{J_0 \hat{\eta}}{\sigma_a H h} \tag{28}$$

where $D = \partial/\partial y$. In (26), χ_a can be eliminated using (27), which reduces the stability problem to two ordinary differential equations

$$\left\{ \left(\frac{g\triangle\rho}{\bar{\rho}k^2} \right)(D^2 - k^2) + c^2 - 2cU_0 \left(\frac{\rho_a}{\bar{\rho}H} \right) + U_0^2 \left(\frac{\rho_a}{\bar{\rho}H} \right) \right\} \hat{\eta} = 0 \tag{29}$$

$$\sigma_{\rm a} H h (D^2 - k^2)\hat{\phi} + J_0 \hat{\eta} = 0 \tag{30}$$

and the boundary conditions

$$g \triangle \rho D\hat{\eta} - ik\sigma_{\rm a} B_0 \hat{\phi} = D\hat{\phi} = 0 \qquad \text{at } y = 0 \text{ and } y = L. \tag{31}$$

The stability problem (29)–(31) determines the complex wave speed $c(U_0, B_0, J_0, k) = c_r + ic_i$ of stable ($c_i < 0$) or unstable ($c_i > 0$) perturbations. The condition $c_i(U_0, B_0, J_0, k) = 0$ corresponds to the marginal stability state.

1.4. Non-dimensional parameters. We convert the stability problem (29)–(31) to a non-dimensional form by introducing new variables $y_*, k_*, D_*, c_*, \hat{\eta}_*, \hat{\phi}_*$ via $y_* = y/H$, $k_* = kH$, $D_* = HD$, $c_* = c/c_0$, $\hat{\eta}_* = \eta/H$, $\hat{\phi}_* = \hat{\phi}\sigma_{\rm a} h/(H^2 J_0)$. Here $c_0 = \sqrt{g(\rho_{\rm a} - \rho_{\rm c})/(\rho_{\rm a}/H + \rho_{\rm c}/h)}$ is the propagation speed of internal gravity waves on the interface. Upon introduction of these new quantities into the stability problem, the following dimensionless parameters appear.

$$M = \frac{U_0}{c_0}$$

is the dimensionless velocity of the mean flow.

$$N = \frac{J_0 B_0 H}{(\rho_{\rm a} - \rho_{\rm c}) g h}$$

is the main stability parameter. It describes the ratio between destabilizing electromagnetic forces and stabilizing influence of gravity. The parameter

$$\xi = \frac{1}{1 + \dfrac{\rho_{\rm c} H}{\rho_{\rm a} h}}$$

contains the thicknesses of the fluid layers and densities of the fluids. Finally,

$$A = \frac{L}{H}$$

is the aspect ratio. After rearrangement and dropping the asterisk, the stability problem takes the dimensionless form

$$[(D^2 - k^2) + k^2(c^2 - 2cM\xi + M^2\xi)]\hat{\eta} = 0, \tag{32}$$

$$(D^2 - k^2)\hat{\phi} + \hat{\eta} = 0 \tag{33}$$

with the boundary conditions

$$D\hat{\eta} - iNk\hat{\phi} = D\hat{\phi} = 0 \qquad \text{for } y = 0 \text{ and } y = A. \tag{34}$$

Our goal is to compute the dispersion relation $c(M, N, \xi, A, k)$. In the following consideration we use only the dimensionless variables and drop the asterisk.

2. Solution of the stability problem.

2.1. The general case: interaction between MHD-instability and Kelvin–Helmholtz instability. Let us introduce the following abbreviations

$$\kappa^2 = k^2(c^2 - 2\xi Mc - 1 + \xi M^2), \quad p = \kappa A/2, \quad q = kA/2 \tag{35}$$

and write the phase velocity of perturbations as

$$c = \xi M \pm \sqrt{1 - M^2(\xi - \xi^2) + \kappa^2/k^2}. \tag{36}$$

Then stability system (32)–(34) becomes

$$(D^2 + \kappa^2)\hat{\eta} = 0, \tag{37}$$

$$(D^2 - k^2)\hat{\phi} + \hat{\eta} = 0, \tag{38}$$

$$D\hat{\eta} - ikDa\hat{\phi} = D\hat{\phi} = 0 \qquad \text{for } y = \pm A/2. \tag{39}$$

Here, we have shifted the y-coordinate in such a way that the centerline of the channel is located at $y = 0$. The general solutions of (37) and (38) are

$$\hat{\eta} = C_1 \cos \kappa y + C_2 \sin \kappa y, \tag{40}$$

$$\hat{\phi} = \frac{C_1 \cos \kappa y}{\kappa^2 + k^2} + \frac{C_2 \sin \kappa y}{\kappa^2 + k^2} + C_3 \cosh ky + C_4 \sinh ky, \tag{41}$$

where C_1, C_2, C_3, C_4 denote unknown coefficients. We apply boundary conditions (39) and obtain a system of four linear equations with four unknown variables C_1, C_2, C_3, C_4. After some algebraic transformation, it can be reduced to

$$\underbrace{\begin{pmatrix} \kappa \sin p & \dfrac{iN}{\kappa^2 + k^2}[k \sin p - \kappa \cos p \, \tanh q] \\ \dfrac{iN}{\kappa^2 + k^2}[k \cos p + \kappa \sin p \, \coth q] & \kappa \cos p \end{pmatrix}}_{Q} \begin{pmatrix} C_1 \\ C_2 \end{pmatrix} = 0 \tag{42}$$

This system has a non-trivial solution only if the determinant of the matrix Q is equal to zero. We find the corresponding value of κ numerically, varying κ and calculating $\det[Q]$ at a given N. After the eigenvalue is found, we use (36) to obtain the complex velocity $c(M, N, \xi, A, k) = c_r + ic_i$ of stable ($c_i < 0$) or unstable ($c_i > 0$) oscillations.

For the states of marginal stability ($c_i = 0$), we obtain the expressions for the interface shape $\eta(x, y, t)$ and the electrical potential perturbation $\phi(x, y, t)$ as

$$\Re\mathrm{e}\,[\eta(x, y, t)] = \Re\mathrm{e}\,\{\hat{\eta}(y) \exp[ik(x - ct)]\}, \tag{43}$$

$$\Re\mathrm{e}\,[\phi(x, y, t)] = \Re\mathrm{e}\,\{\hat{\phi}(y) \exp[ik(x - ct)]\}, \tag{44}$$

where $\hat{\eta}(y)$ and $\hat{\phi}(y)$ are the corresponding eigensolutions (40) and (41).

2.2. The particular case of a pure Kelvin–Helmholtz instability ($N = 0$). In the case of $N = 0$ (which corresponds to $J_0 = 0$ or $B_0 = 0$), we deal with a pure Kelvin–Helmholtz instability. The destabilizing Lorentz forces are non-existent in this case. The mean flow becomes unstable if its velocity exceeds a certain critical value. Here, we will obtain an analytical expression for the critical mean flow velocity.

Inserting $N = 0$ in system (42), we obtain the equation for κ

$$\kappa^2 \sin(2p) = 0, \tag{45}$$

whose solutions are

$$\kappa = \pi n/A \qquad n = 0, 1, \ldots. \tag{46}$$

The complex velocity of perturbations can be easily obtained from equation (36) as

$$c = \xi M \pm \sqrt{1 - M^2(\xi - \xi^2) + \frac{\pi^2 n^2}{k^2 A^2}} \tag{47}$$

We define the critical mean flow velocity M_{cr} as the smallest M, for which the instability appears for an arbitrary wavenumber k. It is clear from the last equation that M_{cr} is to be computed by setting $n = 0$ as

$$M_{\mathrm{cr}} = \sqrt{\frac{1}{\xi - \xi^2}}. \tag{48}$$

2.3. The particular case of a pure MHD instability ($M = 0$). The case of pure MHD-instability corresponds to the situation of a zero mean flow ($M = 0$) when the fluids are initially at rest. In this case, equation (36), which determines the complex speed of interfacial perturbations, simplifies to

$$c = \pm\sqrt{1 + \kappa^2/k^2} \tag{49}$$

The complex parameter κ has to be computed numerically from the condition $\det[\mathrm{Q}] = 0$ [cf. Eq. (42)]. From the condition of instability $\Im\mathrm{m}\,[c] > 0$ it is clear that the instability sets in, if the parameter κ has non-zero imaginary part. Real κ corresponds to stable states. We investigated the stability numerically, starting with stable state (real values of κ for all wavenumbers k) at $N = 0$ and increasing N so that we could find the critical parameter N_{cr}, at which κ moves off into the complex plane. As discussed in the next section, N_{cr} was obtained at $k \to 0$, i.e, the most unstable waves were infinitely long waves.

3. Results. The results of the stability analysis described in this section can be summarized as follows. Both the mean flow and the electromagnetic fields can trigger its own instability, but neither of them affects the threshold of instability caused by the other mechanism. The only mutual impact is through the modification of the phase velocity of unstable and stable modes.

3.1. General case: MHD-Instability and Kelvin–Helmholtz instability. It is discussed in the last section that the instability develops through two different mechanisms: the Kelvin-Helmholtz instability and the MHD instability. The main parameter of the Kelvin-Helmholtz instability is a non-dimensional critical mean flow velocity M_{cr}. The main parameter of the MHD instability is N_{cr}. The basic state is stable, if $N < N_{\mathrm{cr}}$ and $M < M_{\mathrm{cr}}$, and unstable otherwise. The main result is that the both stability limits are independent, i.e., M_{cr} does not depends on N and N_{cr} does not depends on M. We can explain this fact as follows. The instability sets in, if the complex part of the phase velocity of perturbations, which is determined by Eq. (36), becomes negative. It can happen only if $M > M_{\mathrm{cr}}$ or κ is complex. The eigenvalues κ are real at small N (at $N = 0$ they are

computed analytically, see Eq. (46)) and then with the increase of N they move off into the complex plane (at $N = N_{\mathrm{cr}}$). It can be also seen from system (42) that κ depends only on N and does not depend on M. Therefore, N_{cr} is independent on M. On the other hand, M_{cr}, which is given by (48), does not depend on N. We conclude that the stability limits M_{cr} and N_{cr} are independent of one another.

Fig. 2*a* shows a stability chart. The marginal stability curve consists of two independent stability thresholds, $N = N_{\mathrm{cr}}$ and $M = M_{\mathrm{cr}}$. Each inner point in the region $N < N_{\mathrm{cr}}$ and $M < M_{\mathrm{cr}}$ means the stability contrary to the outer points, which mean the instability. The stability threshold N_{cr} depends on the aspect ratio A and was computed numerically. M_{cr} was computed from Eq. (48) and depends on the parameter ξ. It can also be seen in Fig. 2*a* that with the increase of the aspect ratio A (corresponding to the increase of the channel width) the stability region decreases. It means that under other equivalent conditions the waves in a narrow channel are more stable than waves in a wide channel. Another possible reason for the contraction of the stability region is the decrease of ξ, which can be caused by an increase of the ratio H/h, where H is the aluminum depth and h is the cryolite depth.

The mean flow plays not only a destabilizing role in our model, but it also modifies the frequencies of the interfacial waves. Fig. 2*b* shows the frequencies of the interface oscillations at different mean flow velocities. At $M = 0$, two

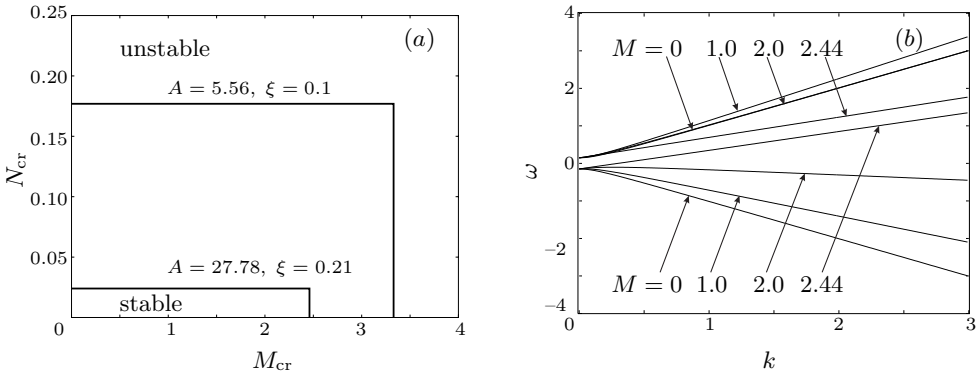

Fig. 2. Stability results for the general case. (a) Stability chart for selected values of ξ and A. (b) Frequencies of interface perturbations for different values of M in the state of marginal stability. $\xi = 0.2132$, $A = 14.95$.

symmetrical waves move in opposite directions. With the increase of M, one of the waves changes its travelling direction to opposite. For large M, both waves move in the same direction as the mean flow.

3.2. The particular case of a pure Kelvin–Helmholtz instability. For $M < M_{\rm cr}$, Eq. (47) gives only real solutions, which describe two stable waves, moving upstream or downstream respectively. With the increase of the mean flow velocity, as M exceeds $M_{\rm cr}$, one of the waves changes its propagation direction. Fig. 3a shows the marginal stability curves for the two modes with transverse wavenumbers $n = 0$ and $n = 1$. The mode with $n = 0$ depends only on x, while the mode with $n = 1$ depends on the both coordinates x and y (cf. inserts). We see that the one-dimensional mode ($n = 0$) is the most unstable mode for any wavenumber k and the critical mean flow velocity $M_{\rm cr}$ is defined by the stability of the mode with $n = 0$ and is given by Eq. (48).

Instability limits with respect to higher modes with $n \geq 1$ depend on the longitudinal wavenumber k [see Fig. 3a]. For these modes short waves are more unstable than long waves.

Figure 3b shows the frequencies of the interface oscillations in the marginal

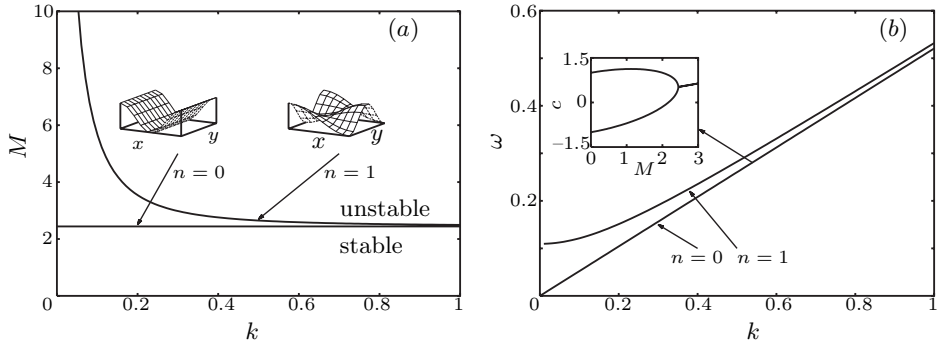

Fig. 3. Stability results for the particular case of a pure Kelvin–Helmholtz instability ($N = 0$). (a) Marginal stability curves for the two first transverse modes: $n = 0$ and $n = 1$. The inserts show the interfaces for $0 < x < 2L$, $0 < L < y$. (b) Frequency of interface perturbations ω in the marginally stable state ($M = M_{\rm cr}$) as a function of longitudinal wavenumber k and for $\xi = 0.2132$, A=14.95. The insert shows the wave speed as a function of M for $k = 0.5$.

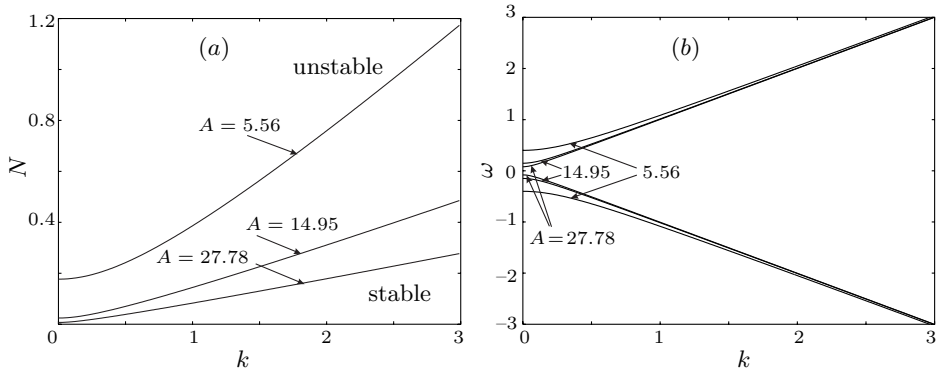

Fig. 4. Stability results for the particular case of a pure MHD-instability ($M = 0$). (a) Marginal stability curves for different aspect ratios A. (b) Frequencies of interface perturbations in the marginal stability state.

stability state, at $M = M_{\rm cr}$.

3.3. The particular case of a pure MHD instability. This case (characterized by $M = 0$) was considered by Davidson & Lindsay [12]. However, the dependence of $N_{\rm cr}$ on ξ and A was not discussed there. Fig. 4 illustrates the family of stability curves for different aspect ratios A as obtained from our numerical computation. The instability sets in at the threshold value of N that depends on the wavenumber k. Our computations show that for the MHD-instability short waves are more stable if compared to long waves.

An increase of the aspect ratio A leads to the reduction of the instability threshold for all k. It can be shown that for $A \to \infty$ (only one wall), $N_{\rm cr} \to 0$.

4. Summary and conclusions. We have presented a simplified model of an aluminum reduction cell with an uniform mean flow in an aluminum layer. Two major sources of instability, namely, the Kelvin–Helmholtz instability and MHD-instability, are investigated.

The Kelvin–Helmholtz instability is characterized by the critical mean flow velocity $M_{\rm cr}$, given by Eq. (48), at which transition to the unstable state occurs. At $M = M_{\rm cr}$ the one-dimensional mode with a transverse wavenumber $n = 0$ (depending only on x) becomes unstable, while the modes with $n > 0$ are destabilized at higher M. For the one dimensional mode, the instability sets in for all k at the same value of M, whereas, for the two-dimensional modes the stability threshold depends on k. Long waves are more stable in comparison with the short ones. The critical mean flow velocity $M_{\rm cr}$ depends only on the densities of the fluids and the layer thicknesses. If the densities of fluids are close to one another (as is the case of the aluminum reduction cells), the waves are more stable in the channel with deep aluminum in comparison with the channels, where this layer is shallow.

The parameter N is the criterion for the onset of the MHD-instability. For small values of N the waves are stable and become unstable as soon as N exceeds the critical value that depends on k. In contrast to the Kelvin–Helmholtz instability, the short waves are more stable in comparison with the long waves. The aspect ratio A influences the stability. The waves in a wide channel are more unstable in comparison with a narrow channel.

We have not observed any cross-interference between the mechanisms of the MHD and Kelvin–Helmholtz instabilities, as far as the threshold of instability is concerned. Both effects occur independently of one another. However, the direction of propagation of the interfacial waves is influenced by the mean flow.

For $M = 0$, there exist two symmetrical waves, moving in opposite directions. At $M > 0$, one of the waves slows down and then changes its travelling direction so that for large values of M, both waves move in the direction of the mean flow.

The present stability analysis in an infinite channel is the first step toward the understanding of the role played by the mean flow in the aluminum reduction cells. In the future investigations we plan to solve the same stability problem in a more realistic geometry, namely, in the rectangular box.

Acknowledgements. This work was partially supported by the Deutsche Forschungsgemeinschaft in the framework of "Forschergruppe Magnetofluiddynamik" (Grant No. FOR 421). One of the authors (O. Z.) was partially supported by the US Department of Energy (Grant DE-FC36-02ID14398). The authors thank P.A. Davidson for useful discussions.

REFERENCES

[1] T. Sele. Instabilities of the metal surface in electrolytic alumina reduction cells. *Met. Trans.*, vol. 8B (1977), pp. 613–618.

[2] R.J. Moreau, D. Ziegler. Stability of aluminum cells – a new approach. *Ligth Metals*, (1986), pp.359–364.

[3] N. Urata. Magnetics and metal pad instability. *Light Metals*, (1985), pp. 581–589.

[4] Ch. Droste, M. Segatz, D. Vogelsang. Improved 2-dimensional model for magnetohydrodynamic stability analysis in reduction cells. *Light Metals*, (1998), pp.419–428.

[5] M. Segatz, C. Droste. Analysis of magnetohydrodynamic instabilities in aluminum reduction cells. *Light Metals*, (1994), pp. 313–322.

[6] V. Bojarevics, M.V. Romerio. Long waves instability of liquid metal-electrolyte interface in aluminum electrolysis cells a generalisation of Seles criterion. *Eur. J. Mech. B/Fluids*, vol. 13 (1994), no. 1, pp. 33–56.

[7] A.D. Sneyd, A. Wang. Interfacial instability due to MHD mode coupling in aluminum reduction cells. *J. Fluid Mech.*, vol. 263 (1994), pp. 343–359.

[8] P.G. Drazin, W.H. Reid. *Hydrodynamic stability* (Cambridge University Press, Cambridge, 1981).

[9] S. Chandrasekhar. *Hydrodynamic and hydromagnetic stability* (Dover Publications, New York, 1981).

[10] J. Pedlosky. *Geophysical Fluid Dynamics* (Springer-Verlag, New-York, 1987).

[11] O. Zikanov, A. Thess, P.A. Davidson, D.P. Ziegler. A new approach to numerical simulation of melt flows and interface instability in Hall–Heroult cells. *Met. Trans.*, vol. 31B (2000), pp. 1541–1543.

[12] P. Davidson, R. Lindsay. Stability of interfacial waves in aluminum reduction cells. *J. Fluid Mech.*, vol. 32 (1998), pp. 273–295.

Received 14.01.2004